

On the First-principles Density Functional Theory Calculation of Electromigration Resistance Ability for Sn-based Intermetallic Compounds

Wen-Hwa Chen^{1,2}, Ching-Feng Yu¹ and Hsien-Chie Cheng^{2,3}

Abstract: The aim of the study is to investigate the interactions between Sn adatoms in a solder bump and three typical Sn-based intermetallic compounds (IMCs) surface, i.e., Cu_3Sn , Cu_6Sn_5 , and Ni_3Sn_4 , at the atomistic scale. The adsorption energy, average bond length, and bond population of the Sn/ Cu_3Sn , Sn/ Cu_6Sn_5 , and Sn/ Ni_3Sn_4 systems are calculated through the first-principles density functional theory (DFT) calculation to investigate how the Sn adatoms influence the IMC surface. The calculated results show that the Sn atoms on the Cu_3Sn (0 0 1) surface hold the largest adsorption energy, average bond length and bond population, implying that the Cu_3Sn (0 0 1) surface is the most stable surface for Sn adatoms. Moreover, the electromigration resistance ability of three typical Sn-based IMCs can be further identified according to the nominal the adsorption energy, average bond length, and bond population, which are estimated through averaging the adsorption energy, average bond length, and bond population for the Cu_3Sn , Cu_6Sn_5 and Ni_3Sn_4 IMCs at seven crystal surfaces, i.e., (1 0 0), (0 1 0), (0 0 1), (1 1 0), (1 0 1), (0 1 1) and (1 1 1). The results reveal that Cu_3Sn holds the best electromigration resistance ability, followed by Ni_3Sn_4 and Cu_6Sn_5 .

Keywords: Intermetallic compound, Density functional theory, Electromigration.

1 Introduction

The electromigration is a mass transport phenomenon, in which, metal atoms migrate along the direction of electron flux [Iwasaki and Miura (2003); Gerstle, Silling, Read, Tewary, and Lehoucq (2008)]. This directional diffusion would lead to the

¹ Department of Power Mechanical Engineering, National Tsing Hua University, Hsinchu, Taiwan, ROC.

² Corresponding author.

³ Department of Aerospace and Systems Engineering Feng Chia University, Taichung, Taiwan, ROC.

formation of hillocks at the anode side and voids at the cathode side of the solder. This phenomenon can induce the signal delay, distortion or even short-circuit failure for electronic component under long-firing operation, thereby leading to a decrease of the electronic component reliability. In addition, the current density can be significantly increased as dimension of the solder becomes smaller, thus resulting in a significant current crowding effect. The current effect is a nonhomogeneous distribution of current density, which can remarkably enhance the electromigration phenomenon of the solder.

The electromigration issue on the solder joints through experimental approach has been investigated. For example, Gan and Tu (2005) investigated the polarity effect of electromigration on kinetics of IMC formation at the anode and the cathode in solder. In the study, V-groove solder line samples, with width of 100 μm and length of 500-700 μm , were applied to study interfacial IMC growth between Cu electrodes and Sn-3.8Ag-0.7Cu solder under different current density and temperature settings. The result exhibited that growth of the IMC layer would be enhanced by electric current at the anode and inhibited at the cathode, and showed that the growth of IMC at the anode had a parabolic dependence on time and the growth rate increased with current density. Zhang, Ou, Huang, Tu, Gee, and Nguyen (2006) present that the Cu-Sn IMCs might have better electromigration resistance ability than the solder since electromigration voids generally form at the interface of solder and IMCs. Chae, Chao, Zhang, Im, and Ho (2007) proposed a numerical method based on simulated annealing to deduce diffusivities and effective charge numbers of Cu and Sn components in Cu_3Sn and Cu_6Sn_5 . Chen and Huang (2008) pointed that Ag_3Sn phase could intercept the Bi migration from the cathode side to the anode side after Ag was doped into Sn-58Bi solder. Zhang, Guo, and Shang (2008) presented that an abnormal polarity effect would be observed after direct current was applied to the Cu/Sn-9Zn/Cu interconnect. The results further showed that IMC at the cathode side was thicker than that at the anode side, which was in contrast to the Cu/In/Cu and Cu/Sn-Pb/Cu interconnects [Yamanaka, Tsukada, and Suganuma (2007)]. Kumar, Yang, Wong, Kripesh, and Chen (2009) evaluated the effect of moderate electric current density on mechanical properties of Ni-P/Sn-3.5Ag/Ni-P and Ni/Sn-3.5Ag/Ni solder joints, and it was found that the electromigration induced brittle failure of the solder joints and this tendency for brittle failure increased with increasing current density. Chen, Huang, and Lin (2009) investigated the electromigration behavior of Cu/Sn-8Zn-3Bi/Cu interconnects. They found that Bi was the dominant migrating species but Sn and Zn were relatively immobile under EM at 80 °C. Wu, Chung, Chen, and Ho (2009) put their focus on evaluating the electromigration effect on the Cu-Ni cross-interaction in Cu/Sn/Ni diffusion couples and showed that the Cu-Ni crossinteraction strongly depended on

the direction of electron flow. Lin, Lin, and Chuang (2009) studied the electromigration behavior of Sn-3Ag-0.5Cu and Sn-3Ag-0.5Cu-0.5Ce-0.2Zn solder joints at room temperature with a current density of 3.1×10^4 A/cm². The evaluated results demonstrated that after doping with Zn and Ce, the electromigration process of Sn-Ag-Cu solder joints was accelerated due to the refinement of the solder matrix. Chen, Huang, and Zhou (2010) adopted the line-type Cu/Sn/Cu interconnections to determine the growth kinetics of interfacial IMCs under current densities ranging from 5.0×10^3 - 1.0×10^4 A/cm² at 100 °C and 150 °C, respectively. The results showed that interfacial IMCs at the anode side were thicker than those at the cathode side. To further enhance the electromigration resistance ability, many elements, such as Cr [Cabral, Harper, Holloway, Smith, and Schad (1992); Sandberg and Holmestad (2006)], Al [Ding, Lanford, Hymes, and Murarka (1994)], Zr [Hu and Luther (1995)] and Ag [Menzel, Strehle, Wendrock, and Wetzig (2005)], had been added into Cu interconnection to increase the diffusion activation energy, thereby improving the electromigration resistance ability. Lee, Hu, and Tu (1995) found that the electromigration activation energy for Cu was 0.73 eV at temperature of 250-450 °C and current density of 5.0×10^5 - 2.1×10^6 A/cm². Nevertheless, the activation energy would increase to 0.95 eV, 1.25 eV and 1.14 eV after alloying Sn with concentrations of 0.5 wt%, 1.0 wt% and 2.0 wt%, respectively. Yan, Suh, Ren, Tu, Vairagar, Mhaisalkar, and Krishnamoorthy (2005) proposed that a 20 nm thick Cu₃Sn IMC on the Cu surface would block the surface diffusion paths, thus resulting in an improvement of electromigration lifetime. Yu, Liu, Lu, and Chen (2007) performed first-principles calculation on evaluating Sn or Cu adatom/Cu (0 0 1), (0 1 0) and (1 1 1) surface systems within local density approximation. They found that the Sn/Cu system was more stable than Cu/Cu system based on the calculated adsorption energy, density of states and electron population analysis.

In literature, the electromigration behaviors of solder joints were well addressed by numerous studies, and the electromigration lifetime would be improved by doping metal elements, such as Cr, Al, Zr, and Ag, in the Cu interconnection. However, it is found that only few studies were made on quantifying the electromigration resistance ability of IMC. In other words, the IMC influence on the electromigration resistance ability of solder bump is not fully understood. Therefore, the alternation goal of the study is to investigate the interactions between Sn adatoms in a solder bump and three typical Sn-based IMCs surface, i.e., Cu₃Sn, Cu₆Sn₅, and Ni₃Sn₄, at the atomistic scale. The adsorption energy, average bond length, and bond population of the Sn/Cu₃Sn, Sn/Cu₆Sn₅, and Sn/Ni₃Sn₄ systems are calculated through the first-principles DFT calculation to investigate how the Sn adatoms influence the IMC surface. These calculations could give guideline for interconnect materials design for an enhanced electromigration resistance ability.

2 Computational details

Seven crystal surfaces, namely (1 0 0), (0 1 0), (0 0 1), (1 1 0), (1 0 1), (0 1 1) and (1 1 1), are studied for each IMC (i.e., Cu_3Sn , Cu_6Sn_5 and Ni_3Sn_4). The surface slab size for Cu_3Sn , Cu_6Sn_5 and Ni_3Sn_4 is $2 \times 2 \times 1.5$, $2 \times 2 \times 1$ and $3 \times 3 \times 1.5$, respectively, and vacuum region is 15 Å, as shown in Figs. 1-3. In specific, a 2×2 surface unit cell with 1.5 slab unit cell thickness is chosen to model the adsorbed surface of Cu_3Sn . For Cu_6Sn_5 and Ni_3Sn_4 , the 2×2 surface unit cell with 1 slab unit cell thickness and 3×3 surface unit cell with 1 slab unit cell thickness are adopted, respectively. The periodic boundary condition is further imposed to the all IMC surface slab. The dimension of these models could ensure that the adatoms can fully relax on the IMC surface but at the same time the computational cost would also be effectively reduced.

In the study, all the simulations are carried out using the first-principles DFT calculation through Cambridge Serial Total Energy Package (CASTEP) code [Payne, Teter, Allan, Arias, and Joannopoulos (1992)]. The Vanderbilt's ultrasoft pseudopotential scheme [Vanderbilt (1990)] is further utilized to model the interactions of valence electrons with ion cores. The exchange-correlation potential is calculated within the GGA using the PBE correlation functional, which depends on both the electron density and its gradient at each space point. The well-known Broyden-Fletcher-Goldfarb-Shanno (BFGS) variable-metric minimization algorithm [Head (1985)] is then utilized to seek the ground state or geometry optimization. It has been demonstrated that the technique is very efficient and robust to explore the optimal minimal energy crystalline structure. The plane wave basis set is truncated using a cutoff energy of 440 eV. To sample the Brillouin zone [Cheng, Yu, and Cheng (2013)], the Monkhorst-Pack kpoint mesh is employed [Monkhorst and Pack (1976)]. It is selected based on the convergence of the k-point mesh, where the change of total energy becomes less than 1 meV/atom [Boukhvalov and Son (2012)]. In the study, the selected k -point mesh is $3 \times 3 \times 1$. The convergence conditions considered in the geometry optimization include an energy tolerance of 2×10^{-5} eV/atom, maximum ionic Hellmann-Feynman force within 0.01 eV/Å, maximum stress within 0.02 GPa and maximum ionic displacement within 5×10^{-4} Å.

3 Results and discussion

3.1 Adsorption energy for Sn adatoms on IMC surface

Adsorption energies are extracted by subtracting the energy of the adsorption system from the energies of Sn adatoms and IMCs surface, as shown in following

equation,

$$E_{ad} = E_{IMC\ surface/Sn} - (E_{IMC\ surface} + E_{Sn}), \quad (1)$$

where $E_{IMC\ surface/Sn}$ is the total energy of Sn adatoms on the IMC surface, $E_{IMC\ surface}$ the total energy of the IMC surface and E_{Sn} the total energy of Sn adatoms. According to the definition, it is noted that a stable adsorption site on a IMC surface can be recognized as the E_{ads} is negative.

Table 1: The adsorption energies (eV) and average bond length, $d_{average}$ (Å), of Sn adatoms on IMC surface versus crystal surface.

IMC type	Crystal surface	$E_{IMC\ surface/Sn}$	$E_{IMC\ surface}$	E_{Sn}	E_{ad}	$d_{average}$
Cu ₃ Sn	(1 0 0)	-1.6417×10^5	-1.6250×10^5	-1.7119×10^3	-4.821	2.920
	(0 1 0)	-7.3739×10^4	-7.2022×10^4	-1.7119×10^3	-5.589	2.825
	(0 0 1)	-7.3732×10^4	-7.2010×10^4	-1.7119×10^3	-10.580	2.721
	(1 1 0)	-7.3999×10^4	-7.2278×10^4	-1.7119×10^3	-8.460	2.779
	(1 0 1)	-9.7448×10^4	-9.5731×10^4	-1.7119×10^3	-5.067	2.879
	(0 1 1)	-1.2803×10^5	-1.2631×10^5	-1.7119×10^3	-5.174	2.856
	(1 1 1)	-9.8146×10^4	-9.6429×10^4	-1.7119×10^3	-4.516	2.964
Cu ₆ Sn ₅	(1 0 0)	-1.5108×10^5	-1.4937×10^5	-1.7119×10^3	-3.645	2.979
	(0 1 0)	-1.5106×10^5	-1.4934×10^5	-1.7119×10^3	-4.869	2.856
	(0 0 1)	-6.2103×10^4	-6.0389×10^4	-1.7119×10^3	-2.604	3.078
	(1 1 0)	-9.7010×10^4	-9.5295×10^4	-1.7119×10^3	-2.817	3.015
	(1 0 1)	-1.8803×10^5	-1.8631×10^5	-1.7119×10^3	-7.052	2.799
	(0 1 1)	-1.8802×10^5	-1.8630×10^5	-1.7119×10^3	-3.666	2.892
	(1 1 1)	-1.1373×10^5	-1.1201×10^5	-1.7119×10^3	-5.218	2.827
Ni ₃ Sn ₄	(1 0 0)	-8.1749×10^4	-8.0029×10^4	-1.7119×10^3	-7.927	2.767
	(0 1 0)	-1.6180×10^5	-1.6009×10^5	-1.7119×10^3	-4.000	2.884
	(0 0 1)	-6.3198×10^4	-6.1484×10^4	-1.7119×10^3	-2.762	3.001
	(1 1 0)	-1.6024×10^5	-1.5853×10^5	-1.7119×10^3	-4.521	2.864
	(1 0 1)	-7.6825×10^4	-7.5107×10^4	-1.7119×10^3	-5.866	2.825
	(0 1 1)	-6.3960×10^4	-6.2244×10^4	-1.7119×10^3	-5.003	2.842
	(1 1 1)	-7.2089×10^4	-7.0377×10^4	-1.7119×10^3	-2.597	3.110

The results obtained for Sn adatoms on IMC surface as a function of crystal surface are shown in Table 1, and their corresponding configurations are demonstrated in Figs. 1-3. From Table 1, it is evident that Sn adatoms on the Cu₃Sn (0 0 1) surface holds the largest adsorption energy, -10.580 eV, followed by the Cu₃Sn (1 1 0), Cu₃Sn (0 1 0), Cu₃Sn (0 1 1), Cu₃Sn (1 0 1), Cu₃Sn (1 0 0) and Cu₃Sn (1 1 1). This

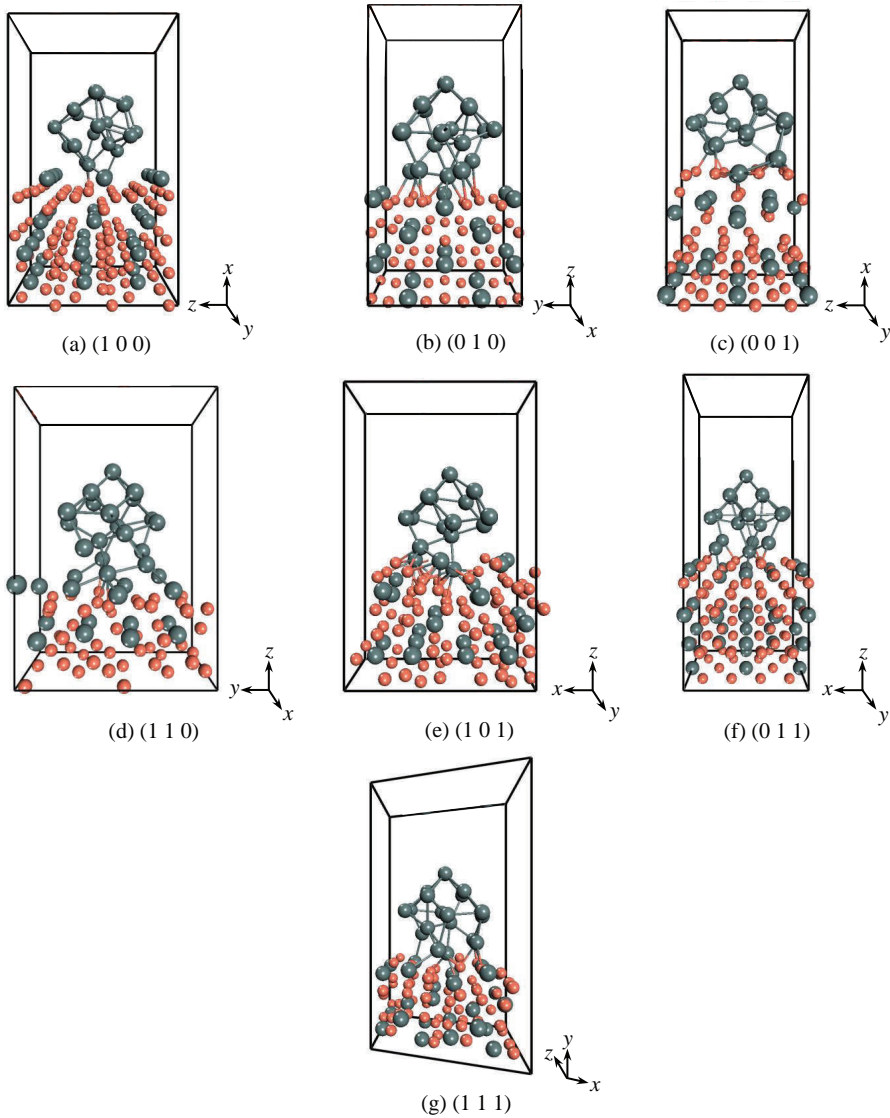


Figure 1: The atomic models of Sn adatoms on Cu_3Sn IMC slab versus crystal surface.

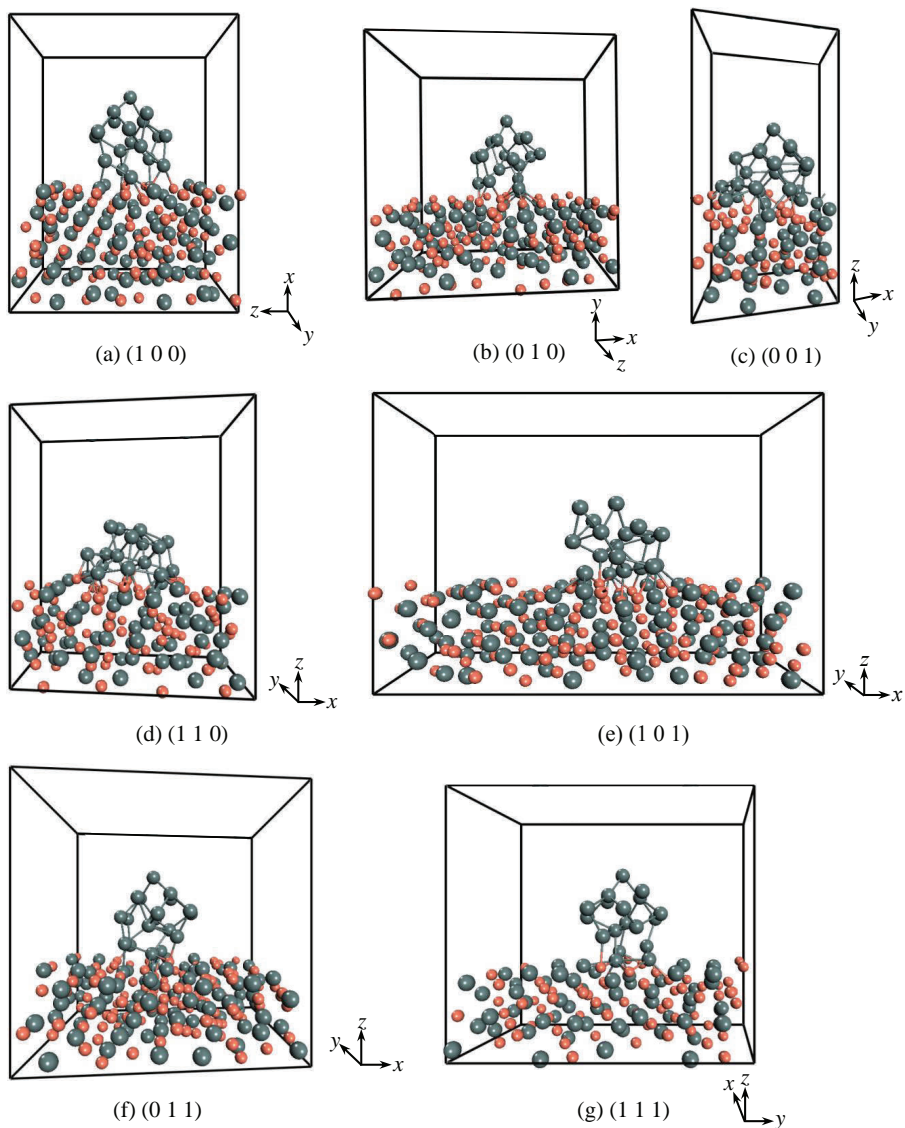


Figure 2: The atomic models of Sn adatoms on Cu₆Sn₅ IMC slab versus crystal surface.

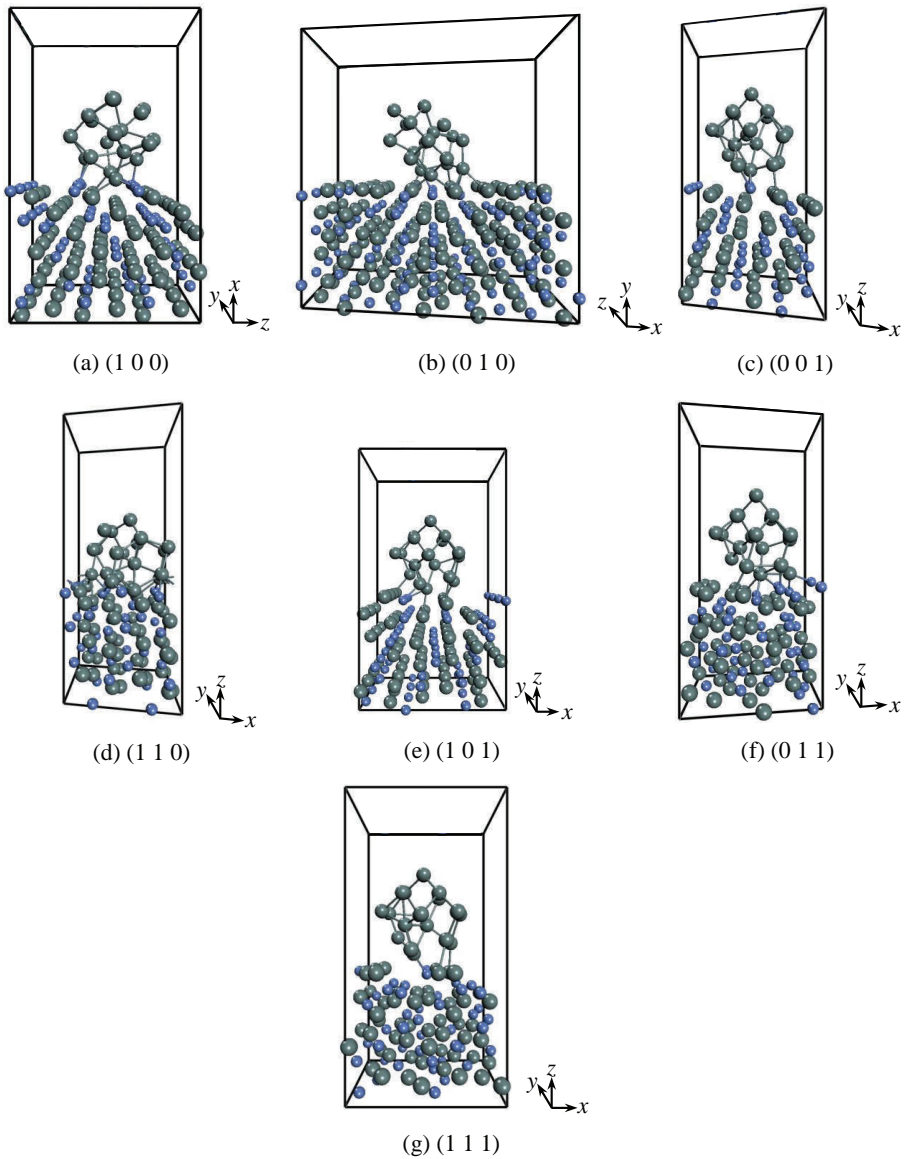


Figure 3: The atomic models of Sn adatoms on Ni_3Sn_4 IMC slab versus crystal surface.

indicates that the Cu_3Sn (0 0 1) surface is the most stable surface for Sn adatoms. For the Cu_6Sn IMC, the (1 0 1) surface is the most stable one for Sn adatoms. Besides, Table 1 also exhibits that Sn adatoms on the Ni_3Sn_4 (1 0 0) surface possesses the largest adsorption energy as compared to that of other crystal surfaces of Ni_3Sn_4 IMC, suggesting that Sn adatoms on the Ni_3Sn_4 (1 0 0) surface can dwell in the most stable state. Consequently, by averaging the adsorption energies of seven crystal surfaces of each IMC (i.e., Cu_3Sn , Cu_6Sn_5 and Ni_3Sn_4), it appears that the average adsorption energies of the Cu_3Sn , Cu_6Sn_5 and Ni_3Sn_4 IMCs are around -6.315 eV, -4.267 eV and -4.668 eV. Notably, the adsorption energies of Cu_3Sn , Cu_6Sn_5 and Ni_3Sn_4 IMCs are all larger than -0.400 eV [Lou, Zhang, Liang, Li, and Zhu (2010); Wang, Han, Hao, Zhang, and Xu (2012)], indicating that the Sn adatoms on the all IMCs surface are categorized as chemical adsorption. Moreover, that the Cu_3Sn IMC has the best electromigration resistance ability among the Sn-based IMC phases. In other words, the Cu_6Sn_5 IMC are more susceptible to electromigration than the Cu_3Sn and Ni_3Sn_4 IMCs. Most importantly, the ranking of the electromigration resistance ability of Sn-based IMCs (i.e., $\text{Cu}_3\text{Sn} > \text{Ni}_3\text{Sn}_4 > \text{Cu}_6\text{Sn}_5$) is also in excellent agreement with the literature experimental results [Chae, Chao, Zhang, Im and Ho (2007); Wang, Shen and Lai (2010)].

3.2 Average bond length for Sn adatoms on IMC surface

As the Sn adatoms are placed on the IMC surface, several Sn-Sn, Sn-Cu and Sn-Ni bonds are developed, and the calculated average bond lengths are listed in Table 1. It is found that the average bond length for Cu_3Sn at the seven crystal surfaces (i.e., (1 0 0), (0 1 0), (0 0 1), (1 1 0), (1 0 1), (0 1 1) and (0 1 1)) is about 2.920 Å, 2.825 Å, 2.721 Å, 2.779 Å, 2.879 Å, 2.856 Å and 2.964 Å. The predicted results are confirmed with the calculated adsorption energy, thereby implying that much higher adsorption energy would induce a much shorter average bond length, resulting in a stronger bonding force. This fact can be also observed in the Cu_6Sn_5 and Ni_3Sn_4 IMCs.

3.3 Bond population analysis for Sn adatoms on IMC surface

Bond population analysis is extensively applied in the electronic structure calculations carried out with linear combination of atomic orbitals (LCAO) basis sets [29]. The total overlap population may be used to provide an objective criterion for bonding between atoms, and also, assess the covalent or ionic nature of a bond. A high value of the bond population indicates a covalent bond, while a low value denotes an ionic interaction. The total overlap populations for all the IMC systems are listed in Table 2. It can be seen that the Sn adatoms on the Cu_3Sn (0 0 1) surface possesses the largest total bond population, which suggests that the bonding abil-

ity of Sn adatoms on the Cu_3Sn (0 0 1) surface is the best among the other Cu_3Sn surfaces. The finding is in agreement with the results for the adsorption energy and average bond length versus crystal surface shown in Table 1. Likewise, the Sn adatoms on the Cu_6Sn_5 (0 0 1) and Ni_3Sn_4 (1 0 0) surfaces would also hold a much larger total bond population as compared to Sn adatoms on the other surfaces, which are also consistent with the calculations for the adsorption energy and average bond length versus crystal surface.

Table 2: The total overlap population of Sn adatoms on IMCs surface as a function of crystal surface.

IMC type	Crystal surface	Total overlap population
Cu_3Sn	(1 0 0)	0.61
	(0 1 0)	1.65
	(0 0 1)	2.74
	(1 1 0)	1.78
	(1 0 1)	0.77
	(0 1 1)	1.34
	(1 1 1)	0.55
Cu_6Sn_5	(1 0 0)	0.60
	(0 1 0)	1.09
	(0 0 1)	0.38
	(1 1 0)	0.51
	(1 0 1)	2.43
	(0 1 1)	0.72
	(1 1 1)	1.54
Ni_3Sn_4	(1 0 0)	2.58
	(0 1 0)	0.95
	(0 0 1)	0.68
	(1 1 0)	1.33
	(1 0 1)	1.58
	(0 1 1)	1.46
	(1 1 1)	0.56

4 Conclusions

In summary, by evaluating the adsorption energy, average bond length and bond population for the Sn atoms in the solder on the crystal surface of the Sn-based

IMCs at different crystal surfaces, the IMCs with better electromigration resistance ability can be characterized. The calculations exhibit that the Sn atoms on the Cu₃Sn (0 0 1) surface possess the largest adsorption energy, average bond length and bond population, suggesting that the Cu₃Sn (0 0 1) surface is the most stable surface for Sn adatoms. Additionally, based on the averaging adsorption energy, average bond length, and bond population for the Cu₃Sn, Cu₆Sn₅ and Ni₃Sn₄ IMCs at seven crystal surfaces, their electromigration resistance ability is further identified. The results reveal that Cu₃Sn holds the best electromigration resistance ability, followed by Ni₃Sn₄ and Cu₆Sn₅, which is consistent with the literature experimental results.

Acknowledgement: The work is partially supported by National Science Council, Taiwan, ROC, under grants NSC101-2221-E-007-009-MY3 and NSC100-2221-E-035-036-MY3. The authors also thank the National Center for High-Performance Computing (NCHC) for computational resources support.

References

- Boukhvalov, D. W.; Son, Y. W.** (2012): Oxygen reduction reactions on pure and nitrogen-doped graphene: a first-principles modeling. *Nanoscale*, vol. 4, pp. 417–420.
- Cabral, C.; Harper, J. M. E.; Holloway, K.; Smith, D. A.; Schad, R. G.** (1992): Preparation of low resistivity Cu-1 at.%Cr thin films by magnetron sputtering. *Journal of Vacuum Science & Technology A*, vol. 10, pp. 1706–1711.
- Chae, S. H.; Chao, B.; Zhang, X.; Im, J.; Ho, P. S.** (2007): Investigation of intermetallic compound growth enhanced by electromigration in Pb-Free solder joints. *Electronic Components and Technology Conference*, pp. 1442–1449.
- Chen, C. M.; Huang, C. C.** (2008): Effects of silver doping on electromigration of eutectic SnBi solder. *Journal of Alloys and Compounds*, vol. 461, pp. 235–241.
- Chen, C. M.; Huang, Y. M.; Lin, C. H.** (2009): Electromigration of Sn-8 wt.% Zn-3 wt.% Bi and Sn-9 wt.% Zn-1 wt.% Cu solders. *Journal of Alloys and Compounds*, vol. 475, pp. 238–244.
- Chen, L. D.; Huang, M. L.; Zhou, S. M.** (2010): Effect of electromigration on intermetallic compound formation in line-type Cu/Sn/Cu interconnect. *Journal of Alloys and Compounds*, vol. 504, pp. 535–541.
- Cheng, H. C.; Yu, C. F.; Chen, W. H.** (2013): First-principles density functional calculation of mechanical, thermodynamic and electronic properties of CuIn and Cu₂In crystals. *Journal of Alloys and Compounds*, vol. 546, pp. 286–295.

- Ding, P. J.; Lanford, W. A.; Hymes, S.; Murarka, S. P.** (1994): Effects of the addition of small amounts of Al to copper: Corrosion, resistivity, adhesion, morphology, and diffusion. *Journal of Applied Physics*, vol. 75, pp. 3627–3631.
- Gan, H.; Tu, K. N.** (2005): Polarity effect of electromigration on kinetics of intermetallic compound formation in Pb-free solder V-groove samples. *Journal of Applied Physics*, vol. 97, p. 063514.
- Gerstle, W.; Silling, S.; Read, D.; Tewary, V.; Lehoucq, R.** (2008): Peridynamic Simulation of Electromigration. *Computer Modeling in Engineering & Sciences*, vol. 8, pp. 75-92.
- Head, J. D.** (1985): A Broyden-Fletcher-Goldfarb-Shanno optimization procedure for molecular geometries. *Chemical Physics Letters*, vol. 122, pp. 264–270.
- Hu, C. K.; Luther, B.** (1995): Electromigration in two-level interconnects of Cu and Al alloys. *Materials Chemistry and Physics*, vol. 41, pp. 1–7.
- Iwasaki, T; Miura, H.** (2003): Molecular-dynamics analysis of grain-boundary grooving in interconnect films with underlayers. *Computer Modeling in Engineering & Sciences*, vol. 4, pp. 551–557.
- Kumar, A.; Yang, Y.; Wong, C. C.; Kripesh, V.; Chen, Z.** (2009): Effect of electromigration on the mechanical performance of Sn-3.5Ag solder joints with Ni and Ni-P metallizations. *Journal of Electronic Materials*, vol. 38, pp. 78–87.
- Lee, K. L.; Hu, C. K.; Tu, K. N.** (1995): In situ scanning electron microscope comparison studies on electromigration of Cu and Cu(Sn) alloys for advanced chip interconnects. *Journal of Applied Physics*, vol. 78, pp. 4428–4437.
- Lin, H. J.; Lin, J. S.; Chuang, T. H.** (2009): Electromigration of Sn-3Ag-0.5Cu and Sn-3Ag-0.5Cu-0.5Ce-0.2Zn solder joints with Au/Ni(P)/Cu and Ag/Cu pads. *Journal of Alloys and Compounds*, vol. 487, pp. 458–465.
- Lou, Z. C.; Zhang, G. Y.; Liang, T.; Li, D.; Zhu, S. L.** (2010): First-principles study on water adsorption on Mg surface. *Journal of Shenyang Normal University*, vol. 28, pp. 189–192.
- Menzel, S.; Strehle, S.; Wendrock, H.; Wetzig, K.** (2005): Effect of Ag-alloying addition on the stress-temperature behavior of electroplated copper thin films. *Applied Surface Science*, vol. 252, pp. 211–214.
- Monkhorst, H. J.; Pack, J. D.** (1976): Special points for Brillouin-zone integrations. *Physical Review B*, vol. 13, pp. 5188–5192.
- Payne, M. C.; Teter, M. P.; Allan, D. C.; Arias, T. A.; Joannopoulos, J. D.** (1992): Reviews of modern physics. *Reviews of Modern Physics*, vol. 64, pp. 1045-1097.
- Sandberg, N.; Holmestad, R.** (2006): First-principles calculations of impurity

diffusion activation energies in Al. *Physical Review B* 73: 014108.

Vanderbilt, D. (1990): Soft self-consistent pseudopotentials in a generalized eigenvalue formalism. *Physical Review B*, vol. 41, pp. 7892–7895.

Wang, C. H.; Shen, H. T.; Lai, W. H. (2010): Effective suppression of electromigration-induced Cu dissolution by using Ag as a barrier layer in lead-free solder joints. *Journal of Alloys and Compounds*, vol. 564, pp. 35–41.

Wang, L. P.; Han, P. D.; Hao, Y. Y.; Zhang, Z. X.; Xu, B. S. (2012): Density functional theory study on Ag adsorption on MgF₂(010) surface. *Chemical Journal of Chinese University*, vol. 33, pp. 569–574.

Wu, W. H.; Chung, H. L.; Chen, C. N.; Ho, C. E. (2009): The influence of current direction on the Cu-Ni cross-interaction in Cu/Sn/Ni diffusion couples. *Journal of Electronic Materials*, vol. 38, pp. 2563–2572.

Yamanaka, K.; Tsukada, Y.; Suganuma, K. (2007): Solder electromigration in Cu/In/Cu flip chip joint system. *Journal of Alloys and Compounds*, vol. 437, pp. 186–190.

Yan, M. Y.; Suh, J. O.; Ren, F.; Tu, K. N.; Vairagar, A. V.; Mhaisalkar, S. G.; Krishnamoorthy, A. (2005): Effect of Cu₃Sn coatings on electromigration life-time improvement of Cu dual damascene interconnects. *Applied Physics Letters*, vol. 87, p. 211103.

Yu, C.; Liu, J.; Lu, H.; Chen, J. (2007): Study of the effects of an adatom Sn on the Cu surface electromigration using a first-principles method. *Applied Surface Science*, vol. 253, pp. 8652–8656.

Zhang, L.; Ou, S.; Huang, J.; Tu, K. N.; Gee, S.; Nguyen, L. (2006): Effect of current crowding on void propagation at the interface between intermetallic compound and solder in flip chip solder joints. *Applied Physics Letters*, vol. 88, p. 012106.

Zhang, X. F.; Guo, J. D.; Shang, J. K. (2008): Growth kinetics of intermetallic compounds between Sn-9Zn solder and electroplated Fe-42Ni metallization. *Journal of Materials Research*, vol. 23, pp. 3370–3378.

